

mice remains to be determined.

If such properties are propagated, then this will suggest that different mutant human PrPs will have generated distinct strains of prions. The existence of prion strains has posed a conundrum as to the mechanism by which strain-specific characteristics are encrypted (23, 26). Although differences in the size of protease-resistant fragments of PrP<sup>Sc</sup> have not been a general characteristic of prion strains (27), the hyper and drowsy strains of prions isolated from mink by serial passage in Syrian hamsters do differ with respect to the size of the PrP<sup>Sc</sup> molecules after limited proteolysis (28). But unlike the studies reported here, where prions were generated de novo in patients carrying the D178N or E200K mutations, the origin of the hyper and drowsy strains is obscure.

Our results provide a plausible mechanism for explaining diversity in a pathogen that lacks nucleic acid; the biological properties of prion strains seem to be encrypted in the conformation of PrP<sup>Sc</sup>. Because prion strains produce different disease phenotypes, such findings raise the possibility that deviations in the phenotypes of other degenerative disorders may also reflect conformational variants in pathologic proteins. Variations in the conformation of PrP<sup>Sc</sup> are reproduced through templating of the PrP<sup>Sc</sup> in the inoculum onto the substrate PrP<sup>C</sup>. Deciphering the molecular events by which the conformation of one protein is imparted to another and the mechanism responsible for the apparently high degree of fidelity associated with this process should be of considerable interest. Indeed, the foregoing data violate the widely and long-held idea that amino acid sequences are the sole determinants of the tertiary structures of biologically active proteins (29).

## REFERENCES AND NOTES

1. D. C. Gajdusek, *Science* **197**, 943 (1977).
2. S. B. Prusiner, *ibid.* **216**, 136 (1982).
3. \_\_\_\_\_, *ibid.* **252**, 1515 (1991).
4. K.-M. Pan *et al.*, *Proc. Natl. Acad. Sci. U.S.A.* **90**, 10962 (1993).
5. S. B. Prusiner *et al.*, *Cell* **35**, 349 (1983); B. W. Caughey *et al.*, *Biochemistry* **30**, 7672 (1991); J. Safar, P. P. Roller, D. C. Gajdusek, C. J. Gibbs Jr., *J. Biol. Chem.* **268**, 20276 (1993); P. Pergami, H. Jaffe, J. Safar, *Anal. Biochem.* **236**, 63 (1996).
6. D. R. Borchelt, M. Scott, A. Taraboulos, N. Stahl, S. B. Prusiner, *J. Cell Biol.* **110**, 743 (1990); N. Stahl *et al.*, *Biochemistry* **32**, 1991 (1993).
7. F. Meggendorfer, Z. Gesmate, *Neurol. Psychiatr.* **128**, 337 (1930); C. L. Masters, D. C. Gajdusek, C. J. Gibbs Jr., *Brain* **104**, 559 (1981).
8. K. Hsiao *et al.*, *Nature* **338**, 342 (1989); M. Poulter *et al.*, *Brain* **115**, 675 (1992); S. R. Dlouhy *et al.*, *Nature Genet.* **1**, 64 (1992); R. B. Petersen *et al.*, *Neurology* **42**, 1859 (1992); R. Gabizon *et al.*, *Am. J. Hum. Genet.* **33**, 828 (1993).
9. R. M. Anderson *et al.*, *Nature* **382**, 779 (1996); G. Chazot *et al.*, *Lancet* **347**, 1181 (1996); R. G. Will *et al.*, *ibid.*, p. 921.
10. G. C. Telling *et al.*, *Proc. Natl. Acad. Sci. U.S.A.* **91**, 9936 (1994).
11. G. C. Telling *et al.*, *Cell* **83**, 79 (1995).
12. S. B. Prusiner *et al.*, *ibid.* **63**, 673 (1990).
13. F. E. Cohen *et al.*, *Science* **264**, 530 (1994).
14. R. Medori *et al.*, *N. Engl. J. Med.* **326**, 444 (1992); L. G. Goldfarb *et al.*, *Science* **258**, 806 (1992).
15. R. B. Petersen, P. Parchi, S. L. Richardson, C. B. Urig, P. Gambetti, *J. Biol. Chem.* **271**, 122661 (1996); R. Riek *et al.*, *Nature* **382**, 180 (1996).
16. J. Tateishi *et al.*, *Nature* **376**, 434 (1995); J. Collinge *et al.*, *Lancet* **346**, 569 (1995).
17. In contrast to Tg(HuPrP) mice, Tg(MHu2M) mice are susceptible to human prions (10). When Tg(MHu2M)Prnp<sup>0/0</sup> mice were produced by crossing onto the PrP null background, a 20% reduction in incubation times was found (11).
18. P. Parchi *et al.*, *Ann. Neurol.* **38**, 21 (1995).
19. L. Monari *et al.*, *Proc. Natl. Acad. Sci. U.S.A.* **91**, 2839 (1994); P. Parchi *et al.*, *Ann. Neurol.* **39**, 767 (1996).
20. G. Telling, N. Heye, S. B. Prusiner, unpublished data.
21. A. Taraboulos *et al.*, *Proc. Natl. Acad. Sci. U.S.A.* **89**, 7620 (1992).
22. V. Manetto *et al.*, *Neurology* **42**, 312 (1992); P. Gambetti, P. Parchi, R. B. Petersen, S. G. Chen, E. Lugaresi, *Brain Pathol.* **5**, 43 (1995).
23. R. Hecker *et al.*, *Genes Dev.* **6**, 1213 (1992).
24. S. J. DeArmond, G. C. Telling, S. B. Prusiner, unpublished data.
25. H. Fraser and A. G. Dickinson, *J. Comp. Pathol.* **83**, 29 (1973); M. E. Bruce, A. G. Dickinson, H. Fraser, *Neuropathol. Appl. Neurobiol.* **2**, 471 (1976); S. J. DeArmond *et al.*, *Proc. Natl. Acad. Sci. U.S.A.* **90**, 6449 (1993).
26. A. G. Dickinson, V. M. H. Meikle, H. Fraser, *J. Comp. Pathol.* **78**, 293 (1968); M. E. Bruce and A. G. Dickinson, *J. Gen. Virol.* **68**, 79 (1987); R. H. Kimberlin, C. A. Walker, H. Fraser, *ibid.* **70**, 2017 (1989); R. I. Carp and S. M. Callahan, *ibid.* **72**, 293 (1991).
27. M. Scott, S. J. DeArmond, S. B. Prusiner, unpublished data.
28. R. A. Bessen and R. F. Marsh, *J. Gen. Virol.* **73**, 329 (1992); *J. Virol.* **68**, 7859 (1994).
29. C. B. Anfinsen, *Science* **181**, 223 (1973).
30. Homogenates (10%, w/v) of human or mouse brain were prepared by repeated extrusion through an 18-gauge syringe needle followed by a 22-gauge needle in phosphate-buffered saline lacking calcium and magnesium ions. For immunoblot analysis, samples were adjusted to 0.5% NP-40 and 0.5% sodium deoxycholate, and samples were digested with proteinase K (PK) (100 µg/ml) for 1 hour at 37°C. Digestion was terminated by the addition of phenylmethylsulfonylfluoride (2 mM final concentration) and boiling in electrophoresis sample buffer (3% SDS, 62.5 mM Tris, pH 6.8). For deglycosylation, the PK-treated samples were digested for 2 hours with recombinant PNGase F (New England Biolabs) as specified by the supplier, precipitated with four volumes of methanol at -20°C, and resuspended in electrophoresis sample buffer.
31. R. J. Kascsak *et al.*, *J. Virol.* **61**, 3688 (1987).
32. T. Muramoto, T. Kitamoto, J. Tateishi, I. Goto, *Am. J. Pathol.* **140**, 1411 (1992).
33. G. C. Telling *et al.*, *Genes Dev.* **10**, 1736 (1996).
34. This work was supported by grants from NIH and the American Health Assistance Foundation, as well as by gifts from the Sherman Fairchild Foundation and the Britton Fund. G.T. was supported by a fellowship from an NIH postdoctoral training grant (NS07219).

23 August 1996; accepted 28 October 1996

## Intestinal Secretory Defects and Dwarfism in Mice Lacking cGMP-Dependent Protein Kinase II

Alexander Pfeifer,\* Attila Aszódi,† Ursula Seidler,† Peter Ruth, Franz Hofmann, Reinhard Fässler

Cyclic guanosine 3',5'-monophosphate (cGMP)-dependent protein kinases (cGKs) mediate cellular signaling induced by nitric oxide and cGMP. Mice deficient in the type II cGK were resistant to *Escherichia coli* STa, an enterotoxin that stimulates cGMP accumulation and intestinal fluid secretion. The cGKII-deficient mice also developed dwarfism that was caused by a severe defect in endochondral ossification at the growth plates. These results indicate that cGKII plays a central role in diverse physiological processes.

Nitric oxide (NO) and a broad spectrum of hormones, drugs, and toxins raise intracellular cGMP concentrations and thereby regulate a great variety of functions, including smooth muscle relaxation, neuronal excitability, and epithelial electrolyte transport (1). Depending on the tissue, the increase in cGMP concentrations leads to the activation of different receptors, such as cyclic nucleotide phosphodiesterases, cGMP-regulated ion channels, and cGK (2). Al-

though the major effects of cGMP have been attributed to the activation of cGK, its physiological role is still controversial (2, 3). It has been suggested that cGMP effects are mediated in some cell types by cross-activation of adenosine 3',5'-monophosphate (cAMP) kinase (cAK) (3), which shares high homology in the cyclic nucleotide binding domains with the cGKs (4). The identification of the physiological mediator of cGMP is further complicated by the existence of two forms of cGK, type I and type II, which are encoded by distinct genes (5). Smooth muscle, platelets, and cerebellum contain high concentrations of the type I cGK, whereas cGKII is highly concentrated in brain, lung, and intestinal mucosa (5, 6). The function of cGKII is not well understood, although there is evidence that it mediates intestinal secretion of water

A. Pfeifer, P. Ruth, F. Hofmann, Institut für Pharmakologie und Toxikologie, Technische Universität München, Biedersteiner Strasse 29, D-80802 München, Germany.

A. Aszódi and R. Fässler, Max-Planck-Institut für Biochemie, D-82152 Martinsried, Germany.

U. Seidler, Medizinische Klinik I, Eberhard-Karls-Universität Tübingen, D-72076 Tübingen, Germany.

\*To whom correspondence should be addressed. E-mail: pfeifer@ipt.med.tu-muenchen.de

†These authors contributed equally to the work.

and electrolyte induced by the *E. coli* toxin STa and the intestinal peptide guanylin (7).

To investigate the physiological roles of cGKII, we generated mice carrying a null mutation of the cGKII gene (cGKII<sup>-/-</sup> mice) (8). The enzyme structure and the targeting vector are shown in Fig. 1A. The deletion of the cGKII gene was confirmed by Northern (RNA) blotting (Fig. 1C), reverse transcriptase-polymerase chain reaction (RT-PCR) (Fig. 1D), and immunoblotting of intestinal, brain, and lung extracts (Fig. 1E). Assays of jejunal homogenates for cGMP-stimulated phosphotransferase activ-

ity (9) confirmed that there was no residual cGKII activity in the mutant mice (Fig. 1G). A deficiency of cGKII had no effect on the integrity of the intestinal cGMP pathway proximal to the kinase, as assayed by STa-stimulated guanylyl cyclase activity (Fig. 1G). Immunoblot analysis indicated that expression of cGKI or the catalytic subunits of cAK was not affected by the absence of cGKII (Fig. 1, E and F). Heterozygous matings of outbred and inbred mice produced viable pups (*n* = 202) with the expected Mendelian frequency. These mice were also fertile as adults, suggesting that embryonic

and fetal development of cGKII-deficient animals was not impaired.

We first tested the effects of cGKII deficiency on intestinal fluid secretion. The cAMP- and cGMP-signaling cascades are key regulators of intestinal chloride and water secretion through the cystic fibrosis transmembrane conductance regulator (CFTR) (3, 7). Some studies have suggested that cGKII mediates the pathophysiological effects of *E. coli* STa (6, 7), a heat-stable enterotoxin that increases cellular cGMP concentrations and induces diarrhea (10), whereas other studies have implicated cross-activation of cAK in these effects (3). We studied electrogenic anion secretion in small intestine and caecum (11) by measuring the short-circuit current (*I*<sub>sc</sub>) of mucosal

**Fig. 1.** Targeted disruption of the cGKII gene. **(A)** Structure of cGKII showing the cGMP-binding pockets (boxed A and B), ATP-binding, and catalytic domain are shown in the top diagram. Localization, restriction map, and organization of exons (filled boxes) and introns (lines) of the cGKII target locus are shown in the second diagram. The targeting vector pNTKK2LS, third diagram, contains 6.2 kb of cGKII genomic sequence that flanks the neomycin resistance cassette (*neo*<sup>r</sup>). The insertion deletes a 308-bp Bam HI–Hinc II fragment of the second coding exon and of the following intron. The disrupted exon (nucleotides 903 to 1070) (5) encodes the first part of the cGMP binding pocket. The bottom diagram shows the structure of the homologous recombination product. Abbreviations: B, Bam HI; R, Eco RV; K, Kpn I; H, Hinc II; S, Sma I; *tk*, herpes simplex virus thymidine kinase gene; and P, probe. **(B)** Identification of cGKII<sup>+/+</sup>, cGKII<sup>+/-</sup>, and cGKII<sup>-/-</sup> mice by Southern (DNA) blot analysis. Hybridization of Eco RV-digested genomic DNA with probe P results in a 3.5-kb mutant-specific band. **(C)** Northern blot of total RNA extracted from the jejunum of cGKII<sup>+/+</sup>, cGKII<sup>+/-</sup>, and cGKII<sup>-/-</sup> mice. The blot was hybridized with mouse cGKII cDNA sequences (nucleotides 690 to 1308) (5). **(D)** RT-PCR (8) of RNA isolated from the small intestine of cGKII<sup>+/+</sup> and cGKII<sup>-/-</sup> mice with primers that amplify cGKII (top) and guanylin (*Gua*) (bottom). **(E)** Immunoblot analysis (8) of cGKII (top) and cGKI (bottom) expression in the duodenum, brain, and lung. **(F)** Immunoblot analysis of cAK expression in duodenum (8). **(G) (Left)** cGMP-stimulated protein kinase activity (9) in the homogenates from mucosal scrapings (BB) of the small intestine. **(Right)** Guanylyl cyclase activity stimulated by STa was determined in brush border membranes isolated from cGKII<sup>+/+</sup> and cGKII<sup>-/-</sup> mice. **(H)** Immunoblots of the BB membranes, used for analysis of kinase activity, and the complete duodenum (Duo), containing the mucosa and the muscularis, which were probed with antibodies to cGKII and cGKI (8).

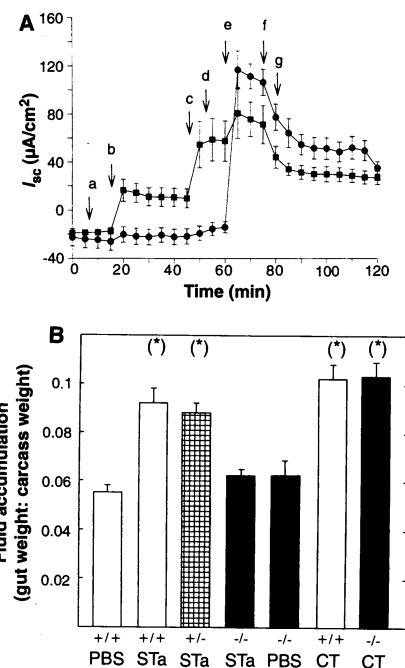
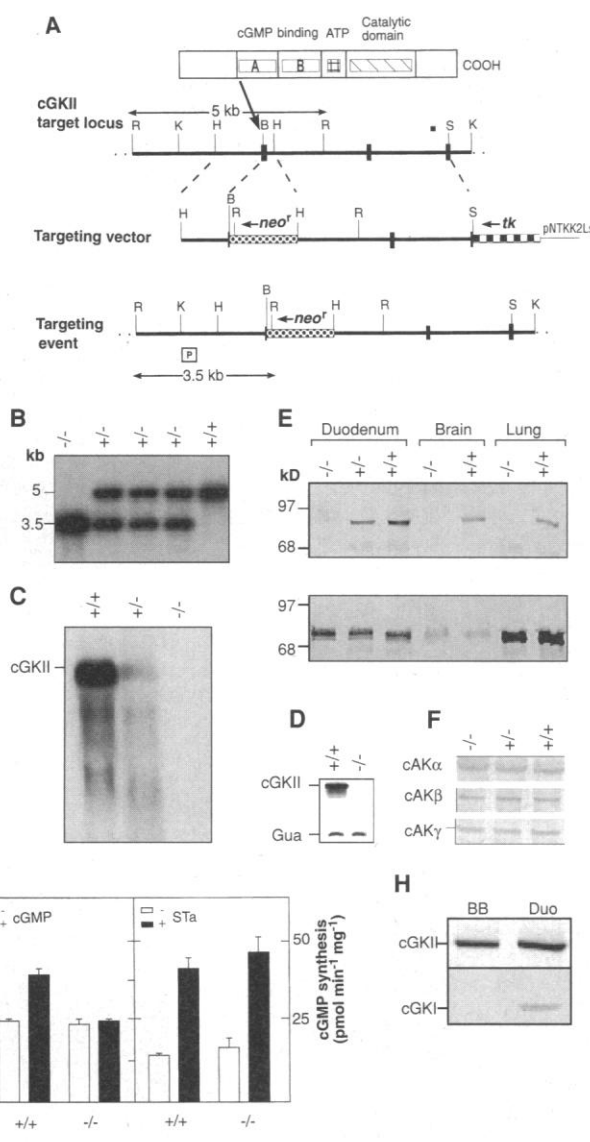


**Fig. 2.** Effect of *E. coli* STa on epithelial electrolyte transport and fluid accumulation in the intestine. **(A)** Epithelial electrolyte transport in stripped mucosa sections from the jejunum of wild-type (v) and cGKII-null (●) mice. The transepithelial electric potential difference was measured in Ussing chamber setups, and the short-circuit current (*I*<sub>sc</sub>) was calculated as in (12). The mucosa sections were treated sequentially with 1 μM tetrodotoxin (a), 100 nM STa (b), 0.2 mM 8-BrGMP (c), 1 mM 8-BrGMP (d), and 1 mM 8-BrAMP (e). Thereafter the tissues were exposed to 100 μM bumetanide (f), which blocks basolateral cotransport of Na<sup>+</sup>, K<sup>+</sup>, and 2Cl<sup>-</sup>, and to 500 μM ouabain (g), which blocks Na<sup>+</sup> and K<sup>+</sup> adenosine triphosphatase. The values are mean ± SEM of five mice for each treatment. **(B)** STa and CT-induced diarrhea in intact mice. Fluid secretion into the intestine was measured as the gut weight: carcass weight ratios in cGKII<sup>+/+</sup>, cGKII<sup>+/-</sup>, and cGKII<sup>-/-</sup> mice after treatment with STa or CT. Controls (PBS) were injected with PBS. (The asterisk indicates *P* < 0.05, Student's *t* test.)

segments (12) treated with STa, cGMP, and cAMP (Fig. 2A). The  $I_{sc}$  of the mouse small intestine is mainly due to CFTR-regulated  $Cl^-$  conductance (13). As expected, treatment of mucosal segments from normal mice with 100 nM STa led to a significant stimulation of  $I_{sc}$  that was further increased by the addition of 0.2 mM and 1 mM 8-bromo-cGMP (8-BrcGMP) (Fig. 2A). Maximum stimulation of  $I_{sc}$  was obtained by superfusion with 1 mM 8-bromo-cAMP (8-BrcAMP). In contrast to

these findings, cGKII-null mice showed only a marginal stimulation of  $I_{sc}$  after STa treatment that was not increased by the addition of 0.2 mM or 1 mM 8-BrcGMP. Jejunal mucosa of cGKII-deficient mice responded normally to 1 mM 8-BrcAMP, demonstrating that the absence of cGKII selectively disrupts the STa-cGMP but not the cAMP pathway.

To evaluate the pathophysiological significance of these observations, we induced secretory diarrhea in newborn mice by in-

tragastric injection of STa (14). Fluid secretion into the intestine of the live animal can be quantified by determining the ratio of gut weight to carcass weight (g/c ratio): g/c ratios greater than 0.083 indicate a diarrheal response, whereas ratios less than 0.074 indicate no response to STa (10). In the cGKII<sup>+/+</sup> and cGKII<sup>+/-</sup> mice, STa induced the accumulation of clear fluid in the intestine, and the g/c ratio increased to  $0.092 \pm 0.006$  ( $n = 5$ ) and to  $0.088 \pm 0.004$  ( $n = 5$ ), respectively (Fig. 2B). In

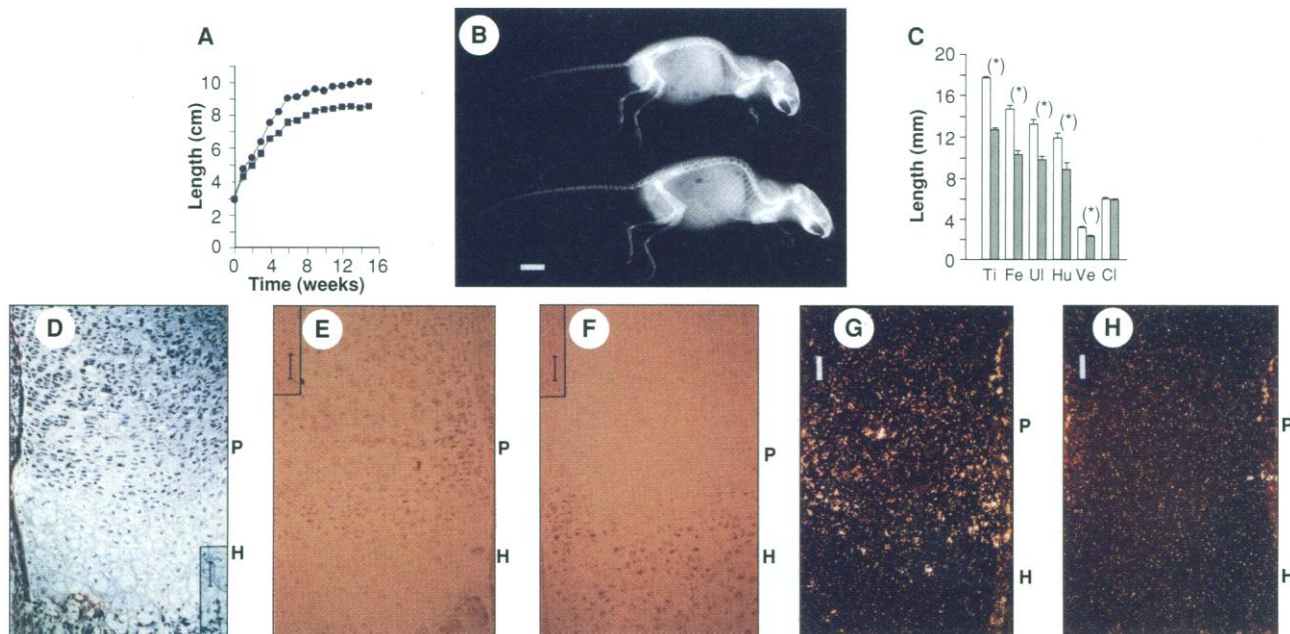


**Fig. 3.** Analysis of the phenotype in bone and of cGK expression in the growth plate (15). **(A)** Time course of body length, measured from the nose to the anus, of cGKII<sup>+/+</sup> (●) and cGKII<sup>-/-</sup> (■) male mice. Female mice showed similar differences (16). The length of cGKII<sup>-/-</sup> mice differed significantly from control mice beginning from the third week ( $P < 0.05$ ,  $n = 7$  to 17 per point). **(B)** X-ray of 8-week-old cGKII-null mouse (top) and normal littermate (bottom). Bar, 1 cm. **(C)** Length of tibia (Ti), femur (Fe), ulna (Ul), humerus (Hu), vertebra (Ve), and clavicle (Cl) of 8- to 10-week-old cGKII<sup>+/+</sup> (open bars) and

cGKII<sup>-/-</sup> (shaded bars) male mice (asterisk indicates  $P < 0.05$  versus control,  $n = 4$ ). **(D)** Hematoxylin-eosin staining of tibia of a newborn mouse (bar, 200  $\mu$ m). **(E and F)** Immunohistochemical analysis of cGK expression in tibial growth plates of a newborn mouse with antibodies to GSKII (E) and cGKI (F) (bar, 200  $\mu$ m). **(G and H)** In situ hybridization of tibial sections from a 16.5-day-old embryo with a cGKII-specific antisense (G) and sense (H) probe. Darkfield illumination; bar, 200  $\mu$ m. P, proliferative zone; H, hypertrophic zone.

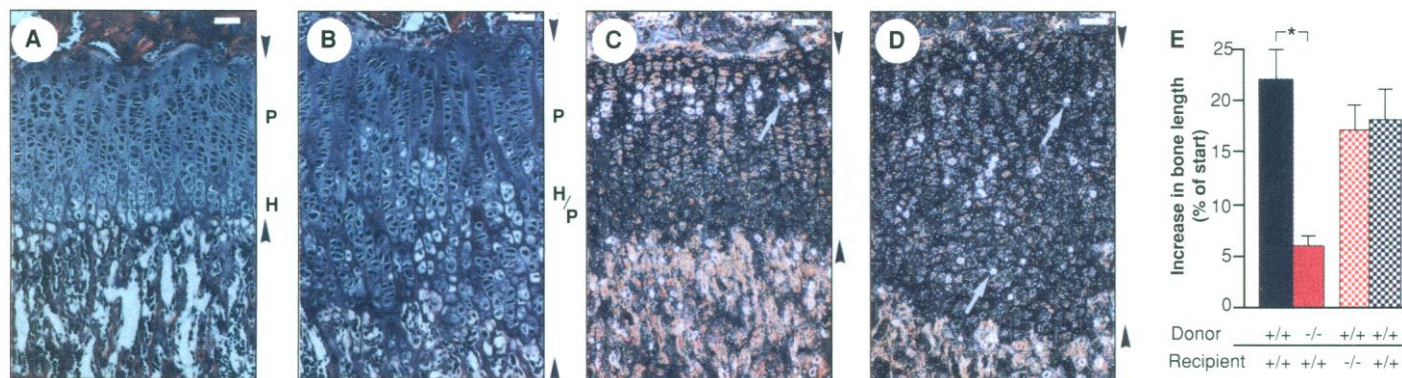


**Fig. 4.** Analysis of the skeletal defect of cGKII-deficient mice. **(A and B)** Sections of the growth plates of tibiae stained with hematoxylin-eosin from 4-week-old wild-type (A) and cGKII-null (B) mice. Zones of proliferative (P) and hypertrophic (H) chondrocytes, as well as the height of the growth plates (arrowheads), are indicated. Bars, 200  $\mu$ m. **(C and D)** [<sup>3</sup>H]Thymidine labeling of proliferative cells (white arrows) in the growth plates of 3-week-old

cGKII<sup>+/+</sup> (C) and cGKII<sup>-/-</sup> (D) mice. The arrowheads indicate the height of the growth plate. Darkfield illumination; bars, 200  $\mu$ m. **(E)** Transplantation of femurs between cGKII<sup>+/+</sup> and cGKII<sup>-/-</sup> inbred mice. The increase in length within 14 days after subcutaneous implantation was measured as percent increase from the start value. Red indicates the data for cGKII<sup>-/-</sup> donors or recipients. An asterisk indicates  $P < 0.05$  versus control ( $n = 6$ ).

contrast, cGKII<sup>-/-</sup> mice showed no accumulation of fluid in the intestine after STa treatment. This lack of response to STa was reflected by a *g/c* ratio of  $0.062 \pm 0.002$  ( $n = 5$ ) (Fig. 2B). However, inactivation of cGKII did not affect the secretory response to agents that raise intestinal cAMP concentrations such as cholera toxin (CT) (Fig. 2B).

As the cGKII<sup>-/-</sup> mice grew, dwarfism, short limbs (micromelia), and cranial abnormalities became apparent. The difference in body length between cGKII<sup>+/+</sup> and cGKII<sup>-/-</sup> mice (15) increased until it reached a constant level at 8 to 10 weeks (Fig. 3A). At this age the mutant mice were 16% shorter and weighed 14% less than their cGKII<sup>+/+</sup> littermates. X-ray analysis (Fig. 3B) and staining of skeletons with alizarin-red (16) revealed a 23 to 30% reduction in the length of the long bones and vertebrae (Fig. 3C). In contrast, the size and weight of the organs within the shortened trunk of cGKII-null mice were normal (16), resulting in a distended abdomen (Fig. 3B). The serum electrolyte levels, bone density, and total body fat (16) of the cGKII-null mice were also normal. These findings, together with the detection of cGKII mRNA in the chondrocytes of the developing bone by *in situ* hybridization (Fig. 3G), suggest that cGKII has a direct role in bone growth.

The normal development of membranous bones like the clavicles (Fig. 3C) and bones of the cranial vault but not of the base of the cranium suggested that the cGKII-null mutation specifically inhibited endochondral but not membranous ossification. During endochondral ossification, bone is deposited on a calcified cartilage matrix that is produced by the growth plate (17). The growth plate is responsible for linear skeletal growth and is characterized by the transition from resting to proliferative to hypertrophic chondrocytes, typically in orderly columnar arrays (17) (Figs. 3D and 4A).

To determine whether growth plate chondrocytes express cGK, we did immunohistochemical stainings with antibodies specific for the two cGK enzymes. Immunohistochemistry for cGKII provided specific staining of a population of chondrocytes located at the border between the proliferative and hypertrophic zone (Fig. 3E). In addition, a weak staining was observed in early proliferative and resting chondrocytes (Fig. 3E). The staining was not present in the cGKII<sup>-/-</sup> animals and also could be competed with purified recombinant cGKII (16). We could also detect cGKI expression in the growth plate that was confined to the hypertrophic zone (Fig. 3F). Preincubation of the cGKI-specific antibody with purified cGKI protein (20

μg/ml) abolished the signal. The cGKI expression pattern and density were not affected by the absence of cGKII (16). *In situ* hybridization studies (Fig. 3, G and H) confirmed the predominant expression of cGKII in the late proliferative and early hypertrophic chondrocytes.

Histological examination of long bones did not reveal substantial abnormalities in newborn cGKII<sup>-/-</sup> mice. Starting at the first week postpartum, the cGKII<sup>-/-</sup> mice developed severe defects in the axial organization of the growth plate, which were most prominent at 3 to 4 weeks of age (Fig. 4B). At this age, cGKII-null mice showed significant changes in growth plate histology consisting of irregular and broadened hypertrophic zones with patches of nonhypertrophic cells intermingled with hypertrophic chondrocytes, even close to the area of vascular invasion. These cells were identified as proliferative chondrocytes by [<sup>3</sup>H]thymidine incorporation (Fig. 4, C and D). In contrast to the wild-type mice (Fig. 4A), the cGKII-null mice showed no clear separation between the proliferative and hypertrophic zone (Fig. 4B). At 6 to 8 weeks of age, cGKII<sup>+/+</sup> and cGKII<sup>-/-</sup> growth plates became smaller, but the mutants showed wedge-shaped columns of mixed hypertrophic and proliferative chondrocytes protruding into the trabecular bone (16).

To exclude the possibility that malabsorption or imbalances in hormones or growth factors were responsible for the retarded growth of the skeleton, we transplanted (15) mutant and normal long bones into normal mice. Whereas the length of normal long bones increased  $23 \pm 4\%$  ( $n = 6$ ), the mutant bones grew only marginally when transplanted into normal mice (Fig. 4E). Furthermore, long bones explanted from wild-type mice developed normally when implanted into cGKII-deficient mice (Fig. 4E). These results suggest that the growth defect in the mutant mice is not due to a general metabolic disturbance.

The phenotype of the cGKII-deficient mice point to a central role for cGKII in diverse physiological processes. The identification of the pathway that mediates intestinal fluid secretion by *E. coli* STa has potential medical implications, because STa causes traveller's diarrhea and about 50% of infant mortality in developing countries (10). Finally the unexpected link between cGKII and bone growth may be an important step for understanding the pathophysiology for a range of bone and joint diseases.

## REFERENCES AND NOTES

- D. L. Garbers and D. G. Lowe, *J. Biol. Chem.* **269**, 30741 (1994); H. H. W. Schmidt and U. Walter, *Cell* **78**, 919 (1994).
- F. Hofmann, W. Dostmann, A. Keilbach, W. Landgraf, P. Ruth, *Biochim. Biophys. Acta*, **1135**, 51 (1992); S. H. Francis and J. D. Corbin, *Annu. Rev. Physiol.* **56**, 237 (1994); T. M. Lincoln and T. L. Cornwell, *FASEB J.* **7**, 328 (1993).
- L. R. Forte *et al.*, *Am. J. Physiol.* **263**, C607 (1992); A. C. Chao *et al.*, *EMBO J.* **13**, 1065 (1994).
- J. B. Shabb and J. D. Corbin, *J. Biol. Chem.* **267**, 5723 (1992).
- W. Wernet, V. Flockerzi, F. Hofmann, *FEBS Lett.* **251**, 191 (1989); M. Sandberg *et al.*, *ibid.* **255**, 321 (1989); M. Uhler, *J. Biol. Chem.* **268**, 13586 (1993); T. Jarchau *et al.*, *Proc. Natl. Acad. Sci. U.S.A.* **91**, 9426 (1994).
- T. Markert *et al.*, *J. Clin. Invest.* **96**, 822 (1995).
- P. J. French *et al.*, *J. Biol. Chem.* **270**, 26626 (1995).
- cGKII DNA was isolated from a genomic library made from 129/Sv mouse tissue (Genome Systems). A 1.4-kb Hinc II-Bam HI and a 4.8-kb Hinc II-Sma I fragment of the cGKII gene was cloned 5' and 3' of the neomycin resistance expression cassette (*neo<sup>r</sup>*). The herpes simplex virus thymidine kinase cassette (*tk*) was cloned 3' to the cGKII sequence. R1 embryonic stem (ES) cells [A. Nagy, J. Rossant, R. Nagy, W. Abramow-Newerly, J. C. Roder, *Proc. Natl. Acad. Sci. U.S.A.* **90**, 8424 (1993)] were electroporated with the linearized vector and plated on irradiated G418-resistant embryonic feeder cells [R. Fässler and M. Meyer, *Genes Dev.* **9**, 1896 (1995)]. Recombinant clones were selected with G418 (0.3 mg/ml) and 1-[2'-deoxy-2'-fluoro-β-D-arabino-furanosyl]-5-iodouracil (FIAU) (0.2 μM). Four of 100 double-resistant colonies showed homologous recombination at the cGKII locus. Germline chimeras were obtained by injection of mutant ES cell clones into C57Bl/6 blastocysts. RT-PCR was performed with primers that amplify cGKII (nucleotides 508 to 1740) (5) and guanylin (nucleotides 331 to 521) [D. Sciaky, J. L. Kosiba, M. B. Cohen, *Genomics* **24**, 583 (1994)], respectively. Immunoblot analysis was performed with antibody (Ab) B32-A3 to the COOH-terminal region of mouse cGKII, Ab A16-14 to cGKI, and Ab to the α, β, and γ catalytic subunits of the cAK (Santa Cruz Biotechnology, Santa Cruz, CA).
- The intestine was removed from freshly killed mice and purged with phosphate-buffered saline (PBS). The epithelial cells were scraped from the mucosal surface and resuspended in 20 mM KH<sub>2</sub>PO<sub>4</sub>, pH 7.0, 2 mM EDTA, and 2 mM benzamide (for kinase determination) or in 10 mM tris-HCl (pH 7.4), 300 mM sorbitol, 2 mM benzamide, and leupeptin (20 μg/ml) (for guanylate cyclase activity). The kinase activity was determined as described [P. Ruth *et al.*, *Eur. J. Biochem.* **202**, 1339 (1991)], with 10 μg of protein and in the presence or absence of 30 μM cGMP. GC activity in brush border membranes was determined as described [A. B. Vaandrager, S. Schulz, H. R. De Jonge, D. L. Garbers, *J. Biol. Chem.* **268**, 2174 (1993)], with 35 μg of protein and 400 ng of STa. The samples were acetylated and cGMP concentrations were determined in an enzyme immunoassay (Cayman, Ann Arbor, MI). Values are expressed as the mean ± SEM with  $n = 8$  for kinase activity and  $n = 4$  for guanylyl cyclase activity.
- R. A. Giannella, *Infect. Immun.* **14**, 95 (1976); *Annu. Rev. Med.* **32**, 341 (1981).
- The midpart of the jejunum was excised and opened longitudinally. All muscle layers were removed with a forceps under the stereomicroscope. The mucosa was mounted between two lucite half-chambers (0.125 cm<sup>2</sup> of exposed area) in an Ussing chamber (World Precision Instruments, Berlin) apparatus. The serosal and luminal solutions were circulated by a gas-lift system and were identical except that indomethacin (10 μM) and glucose (2 mM) were present in the serosal perfusate, and mannitol (2 mM) in the luminal perfusate. The perfusate solutions contained 140.5 mM Na<sup>+</sup>, 4.5 mM K<sup>+</sup>, 2 mM Ca<sup>2+</sup>, 1.3 mM Mg<sup>2+</sup>, 126 mM Cl<sup>-</sup>, 1.3 mM SO<sub>4</sub><sup>2-</sup>, 20 mM HCO<sub>3</sub><sup>-</sup>, and 1.5 mM HPO<sub>4</sub><sup>2-</sup>, were gassed with 5% CO<sub>2</sub>-95% O<sub>2</sub>, and were kept at 37°C.
- H. H. Ussing and K. Zerahn, *Acta Physiol. Scand.* **23**, 110 (1951).
- S. E. Gabriel, K. N. Brigman, B. H. Koller, R. C. Boucher, M. J. Stutts, *Science* **266**, 107 (1994).

14. The suckling mouse model (10) was used to quantify the STa-induced diarrhea in vivo. STa (50 ng) was dissolved in 0.5 ml of isotonic PBS and injected intragastrically in 3- to 4-day-old mice. After a 2-hour incubation at 25°C, the whole intestine without stomach was carefully removed and weighed. The g/c ratio was calculated as the ratio of gut weight to remaining carcass weight. To evaluate the response to CT, we used the sealed mouse model [S. H. Richardson, J. C. Giles, K. S. Kruger, *Infect. Immun.* **43**, 482 (1984)]. Data are expressed as mean  $\pm$  SEM of five mice for each treatment.  $P < 0.05$  versus control.
15. Bone length was determined by x-ray analysis and by analysis of alizarin-red-stained skeletons. Data are expressed as mean  $\pm$  SEM. For immunohistochemistry, knees were fixed in 95% ethanol overnight and cut in 6- $\mu$ m sections. Sections were incu-

bated for 1 hour with Abs to cGKI and cGKII (8). The primary Abs were visualized by using a biotinylated secondary Ab (antibody to rabbit immunoglobulin G), followed by avidin-peroxidase complex and developed with H<sub>2</sub>O<sub>2</sub>-3,3'-diaminobenzidintetrahydrochlorid (Vectastain, Burlinghome, CA). For in situ hybridization, specimens were fixed in 4% paraformaldehyde overnight, embedded in paraffin, and cut in 6- $\mu$ m sections. In situ hybridization was performed with a cGKII cDNA probe (nucleotides 960 to 1719) (5). [<sup>3</sup>H]Thymidine labeling of growth plates was performed as described [A. M. Reimold *et al.*, *Nature* **379**, 262 (1996)], and bone transplantation was performed as described by W. J. L. Felts [*Transplant. Bull.* **4**, 5 (1957)]. Femurs of 1-week-old donors were implanted subcutaneously into 4- to 6-week-old recipients. After 14 days, the mice were killed and the

length of the femurs was determined.

16. A. Pfeifer *et al.*, data not shown.
17. A. Erlebacher, E. H. Filvaroff, S. E. Gitelman, R. Derynck, *Cell* **80**, 371 (1995); E. B. Hunziker, R. K. Schenk, L. M. Cruz-Orive, *J. Bone Jt. Surg.* **69**, 162 (1987).
18. We thank K. Kühn for his advice; M. Walter, M. Guba, and I. Blumenstein for their help in the Ussing chamber experiments; K. Doerr, S. Kamm, and S. Benkert for technical assistance; and P. Klatt for help in quantifying the total body fat of the mice. Supported by grants from the Deutsche Forschungsgemeinschaft, Bundesministerium für Forschung und Technologie, and Fonds der Chemie. R.F. was supported by the Hermann and Lilly Schilling Stiftung.

9 July 1996; accepted 2 October 1996

## Control of EGF Receptor Signaling by Clathrin-Mediated Endocytosis

Amandio V. Vieira, Christophe Lamaze, Sandra L. Schmid\*

Epidermal growth factor receptor (EGFR) signaling was analyzed in mammalian cells conditionally defective for receptor-mediated endocytosis. EGF-dependent cell proliferation was enhanced in endocytosis-defective cells. However, early EGF-dependent signaling events were not uniformly up-regulated. A subset of signal transducers required the normal endocytic trafficking of EGFR for full activation. Thus, endocytic trafficking of activated EGFR plays a critical role not only in attenuating EGFR signaling but also in establishing and controlling specific signaling pathways.

Signaling by ligand-activated receptor tyrosine kinases (RTKs) such as EGFR can elicit a wide range of cell type-specific responses leading to proliferation or differentiation. EGF binding triggers dimerization and trans- or autophosphorylation of the receptor, followed by recruitment and activation of SH2 (src homology domain 2) or PTB (phosphotyrosine binding) domain-containing intracellular signal transducers (1). Ligand binding also triggers the recruitment of EGFR to clathrin-coated pits, followed by internalization of the EGFR-ligand complex and its delivery to lysosomes for degradation (2). Although activated EGFR follows the canonical endocytic pathway (3) during this process of "down-regulation," RTK-specific regulators affecting sorting at both early (4, 5) and late (6, 7) trafficking steps have been identified. Many of these regulators, for example, snx-1 (sorting nexin 1) (6) and phosphatidylinositol 3-kinase (PI-3-kinase) (7), appear to affect sorting of only a subset of RTKs. Why should RTKs have their own repertoire of intracellular trafficking regulators? One possibility is that regulation of trafficking serves to modulate RTK signaling.

To examine whether EGFR endocytosis

and trafficking are important for controlling the signaling pathways and cellular responses to EGF, we examined these events

in cells conditionally and specifically defective in clathrin-dependent receptor-mediated endocytosis (8). The conditional defect in endocytosis is imposed by the regulated expression of the Lys<sup>44</sup>  $\rightarrow$  Ala<sup>44</sup> (K44A) mutant form of dynamin (8), a guanosine triphosphatase that is required for clathrin-coated vesicle formation (9).

Ligand-induced endocytosis of EGFR was potently inhibited in cells overexpressing K44A dynamin (K44A cells) as compared with cells overexpressing comparable amounts of wild-type dynamin (WT cells) (Fig. 1A). In contrast, endocytosis of inactivated EGFR, defined as the basal rate and measured with mAb528 [an antagonistic monoclonal antibody (mAb) to EGFR] as ligand (10), was not significantly affected (Fig. 1A). These data confirm the role of

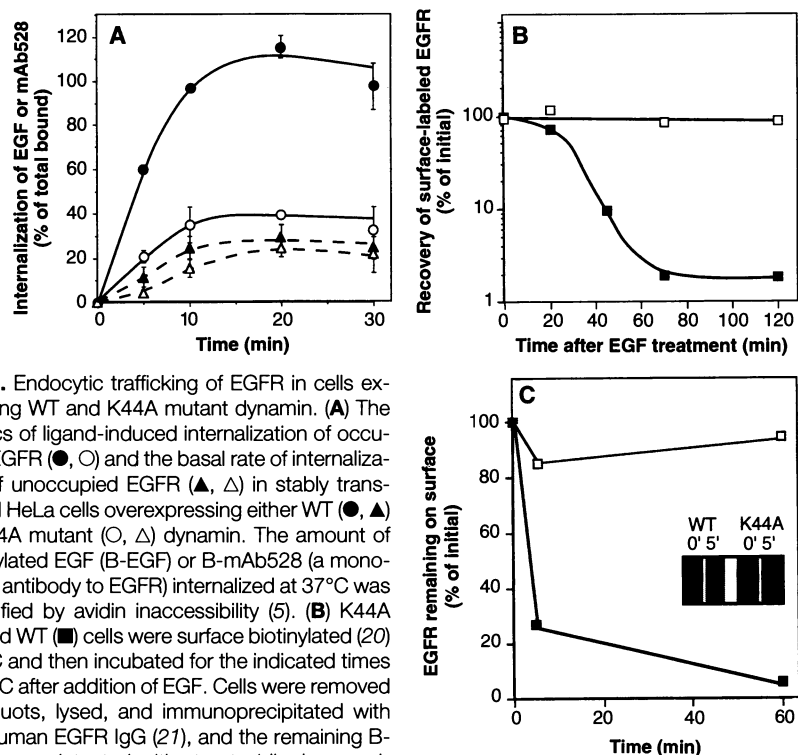


**Fig. 1.** Endocytic trafficking of EGFR in cells expressing WT and K44A mutant dynamin. (A) The kinetics of ligand-induced internalization of occupied EGFR (●, ○) and the basal rate of internalization of unoccupied EGFR (▲, △) in stably transfected HeLa cells overexpressing either WT (●, ▲) or K44A mutant (○, △) dynamin. The amount of biotinylated EGF (B-EGF) or B-mAb528 (a monoclonal antibody to EGFR) internalized at 37°C was quantified by avidin accessibility (5). (B) K44A (□) and WT (■) cells were surface biotinylated (20) at 4°C and then incubated for the indicated times at 37°C after addition of EGF. Cells were removed in aliquots, lysed, and immunoprecipitated with anti-human EGFR IgG (21), and the remaining B-EGFR was detected with streptavidin-horseradish peroxidase. (C) K44A (□) and WT (■) cells were treated with EGF for the indicated times, then surface biotinylated at 4°C (20) and analyzed for B-EGFR after immunoprecipitation (21).

Department of Cell Biology, The Scripps Research Institute, La Jolla, CA 92037, USA.

\*To whom correspondence should be addressed. E-mail: slschmid@scripps.edu